Pergamon

www.neuroscience-ibro.com

PII: S0306-4522(01)00290-1

Neuroscience Vol. 106, No. 4, pp. 733–743, 2001

0306-4522/01 $20.00+0.00

THE SULPHYDRYL REAGENT, *N*-ETHYLMALEIMIDE, DISRUPTS SLEEP AND BLOCKS A1 ADENOSINE RECEPTOR-MEDIATED INHIBITION OF INTRACELLULAR CALCIUM SIGNALING IN THE *IN VITRO* VENTROMEDIAL PREOPTIC NUCLEUS

M. IKEDA,[a,b,c]* M. SAGARA,[b,d] Y. SEKINO,[e] T. SHIRAO,[e] K. HONDA,[b] T. YOSHIOKA,[a,d] C. N. ALLEN[c] and S. INOUÉ[b]

[a]Advanced Research Institute for Science and Engineering, Waseda University, 3-4-1 Okubo, Shinjyuku-ku, Tokyo 169-8555, Japan

[b]Institute of Biomaterials and Bioengineering, Tokyo Medical and Dental University, Tokyo 101-0062, Japan

[c]Center for Research on Occupational and Environmental Toxicology, Oregon Health Sciences University, Portland, OR 97201-3098, USA

[d]School of Human Sciences, Waseda University, Saitama 359-1192, Japan

[e]Department of Neurobiology and Behavior, Gunma University School of Medicine, Maebashi 371-8511, Japan

Abstract—To explore the neuronal signaling mechanisms underlying sleep regulation in the rat, the present study examined continuous intra-third ventricle infusion of *N*-ethylmaleimide (NEM), a sulphydryl reagent that inhibits $G_{i/o}$ protein-coupled receptor-mediated signaling pathways. The diurnal infusion of NEM (0.01–10 μmol/10 h) dose-dependently inhibited both non-rapid eye movement sleep and rapid eye movement sleep. A maximal dose of NEM (10 μmol/10 h) dramatically inhibited day-time sleep (−57% for non-rapid eye movement sleep and −89% for rapid eye movement sleep) with a compensatory increase of sleep during the subsequent night-time (+33% for non-rapid eye movement sleep and +259% for rapid eye movement sleep). The day-time brain temperature was also increased by NEM, demonstrating effects of NEM on both sleep and body temperature levels. Immunostaining of the rat hypothalamus with a monoclonal antibody against the A1 adenosine receptor (A1R) was used to explore the distribution of a sleep-related $G_{i/o}$ protein-coupled receptor. Robust A1R-like immunoreactivity was found in the ventromedial preoptic nucleus and the supraoptic nucleus. Fura-2-based Ca^{2+} imaging analysis of acute hypothalamic slices further demonstrated that the A1R agonist N^6-cyclopentyladenosine (CPA; 200 nM) inhibited spontaneous Ca^{2+} oscillations and high potassium (80 mM)-induced Ca^{2+} flux in the ventromedial preoptic nucleus, while NEM (100–300 μM) and an A1R antagonist 8-cyclopentyl-dipropylxanthine (300 nM) blocked the CPA actions and increased the high potassium-induced Ca^{2+} flux.

From these results we suggest that NEM-sensitive G protein-coupled receptor(s) may play an important role in the regulation of sleep and body temperature in the rat and one possible mechanism is an A1R-mediated regulation of intracellular Ca^{2+} concentrations in the ventromedial preoptic nucleus. © 2001 IBRO. Published by Elsevier Science Ltd. All rights reserved.

Key words: Ca^{2+} imaging, fura-2, GTP-binding protein, immunostaining, intracerebroventricular infusion, voltage-sensitive Ca^{2+} channels.

The neuronal mechanisms that regulate sleep have been extensively studied and a number of neurotransmitters have been described to modulate sleep–wake activities. Receptors coupled to GTP-binding proteins of the $G_{i/o}$ subtypes, such as the A1 adenosine receptor (A1R) (Ticho and Radulovacki, 1991; Schwierin et al., 1996), M2 muscarinic acetylcholine receptor (Imeri et al., 1996), and 5HT-1A serotonin receptor (Monti and Jantos, 1992; Bjorvatn et al., 1997), are proposed to play an important role in the induction of sleep. Indeed, injection, infusion, or micro-dialysis of agonist for these receptors induce non-rapid eye movement sleep (NREMS) and/or rapid eye movement sleep (REMS) depending on the locus of agonist delivery (Virus et al., 1983; Ticho and Radulovacki, 1991; Monti and Jantos, 1992; Imeri et al., 1996; Schwierin et al., 1996; Bjorvatn et al., 1997; Porkka-Heiskanen et al., 1997; Portas et al., 1997; Marks and Birabil, 1998, 2000; Alam et al., 1999; Mendelson, 2000). Since the sleep regulatory system is

*Correspondence to: M. Ikeda, Center for Research on Occupational and Environmental Toxicology, Oregon Health Sciences University, 3181 Sam Jackson Park Road, L606, Portland, OR 97201-3098, USA. Tel.: +1-503-494-2529; fax: +1-503-494-6831.
E-mail address: msikeda@aol.com (M. Ikeda).

Abbreviations: A1R, A1 adenosine receptor; ACSF, artificial cerebrospinal fluid; ANOVA, analysis of variance; CPA, N^6-cyclopentyladenosine; DPCPX, 8-cyclopentyl-dipropylxanthine; EEG, electroencephalogram; EMG, electromyogram; NEM, *N*-ethylmaleimide; NREMS, non-rapid eye movement sleep; PBS, phosphate-buffered saline; REMS, rapid eye movement sleep; TTX, tetrodotoxin; VLPO, ventrolateral preoptic nucleus; VMPO, ventromedial preoptic nucleus; VSCC, voltage-sensitive calcium channel.

very complex and multiple compensatory systems may exist, complete inhibition of sleep by specific receptor antagonists has not been observed. Therefore, it is of interest to determine how sleep is modulated by inhibition of $G_{i/o}$ proteins that couple to the receptors mentioned above.

The sulphydryl alkylator, *N*-ethylmaleimide (NEM), is widely used as an inhibitor of $G_{i/o}$ protein-coupled receptors. NEM uncouples the receptor from the GTP-binding regulatory proteins by alkylating two cysteine residues on the α subunits of $G_{i/o}$ proteins near the site that undergoes an ADP ribosylation by the $G_{i/o}$ inhibitor, pertussis toxin (Asano and Ogasawara, 1985; Winslow et al., 1987). Since the membrane permeability of pertussis toxin peptide is extremely small, extracellular application of pertussis toxin requires overnight treatment and the effects are not reversible. In contrast, NEM is fairly lipophilic and requires only a few minutes to block $G_{i/o}$-mediated signaling. Although NEM also inhibits the activities of several enzymes (Preclik et al., 1992; Cossins et al., 1994; Clottes and Burchell, 1998), NEM has been used as an inhibitor of $G_{i/o}$-mediated signaling both *in vivo* (Sánchez-Blázquez et al., 1989; Garzon et al., 1990) and *in vitro* (Munshi et al., 1991; Shapiro et al., 1994; Barajas-López et al., 1996; Delmas and Gola, 1997; Williams et al., 1997; Lorenzen et al., 1998; Tang and Lovinger, 2000).

We have continuously infused NEM into the third ventricle and demonstrated a significant and reversible inhibition of NREMS and REMS with an increase of brain temperature in freely moving rats. A1R agonists are potent sleep promoters (Schwierin et al., 1996) and our immunohistochemical studies indicated robust A1R-like immunoreactivity in the ventromedial preoptic nucleus (VMPO), a putative regulatory center for sleep and body temperature (Nagel and Satinoff, 1980; Sallanon et al., 1989; Asala et al., 1990; Alam et al., 1995; John and Kumar, 1998). In the present study, we further analyzed the effects of NEM on A1R-mediated inhibition of intracellular Ca^{2+} signaling in the VMPO.

EXPERIMENTAL PROCEDURES

Animals and surgery

Adult male Sprague–Dawley rats (300–450 g, 60–70 days old) from an inbred colony (animal quarters of Tokyo Medical and Dental University) were kept under a 12:12 light:dark cycle at a constant ambient temperature and humidity (25 ± 1°C and 60 ± 6%). Food and water were available *ad libitum*. Animals were anesthetized with an i.p. injection of sodium pentobarbital (50 mg/kg body weight), placed on a stereotaxic apparatus and implanted with three gold-plated stainless steel screw electrodes, placed through the skull on the frontal and occipital cortex, for electroencephalographic (EEG) recording. Two stainless steel hook electrodes were inserted into the cervical portion of the trapezius muscle for electromyographic (EMG) recording. A cortical thermistor probe (G-1E model; Toho Electric Company, Tokyo, Japan) for recording brain temperature was placed in the thalamus at a depth of 4 mm from the skull. To achieve continuous central infusion, an i.c.v. cannula (0.35 mm inner diameter) was inserted into the third ventricle. All electrodes and cannula were permanently affixed to the skull using dental acrylic resin. During and at the end of surgery, a total of 40 000 U of penicillin G potassium (Meiji Pharmaceutical Company, Tokyo, Japan) was subcutaneously and locally applied to the incision. All animal experiments in the present study were approved by the Animal Care and Use Committee at Tokyo Medical and Dental University. Further details of the surgery were described elsewhere (Inoué et al., 1984; Honda et al., 1994; Kimura et al., 2000).

Sleep recordings and continuous i.c.v. infusion

One week was allowed for recovery from surgery. The rats implanted with an i.c.v. cannula were placed into individual sleep-recording cages in a sound-attenuated and electromagnetically shielded chamber. The lead wires of the EEG and EMG electrodes and the brain thermistor were connected to a multiple channel amplifier (MEG-6116; Nihon Kohden, Tokyo, Japan) or to a thermistor amplifier (EC-2390B; Elmec, Tokyo, Japan), via a feed-through slip ring (CAY-675; Airflyte Electronics Company, Bayonne, NJ, USA) fixed above the cage. The EEG, EMG, and thermistor signals were fed into a computer via a high-speed analog-to-digital converter (EC-2390B; Elmec) at a sampling rate of 128 Hz and stored on a magnetic optical diskette. Polysomographic charts were displayed on a high-resolution display (1280×1024 pixels) and sleep–wake stages determined automatically based on the amplitudes of the EEG and EMG. After recordings, the sleep–wake stages were replayed on the monitor and visually re-evaluated by experienced investigators to correct improper scoring of sleep due to artifactual EEG/EMG patterns during wakefulness.

After recovery from surgery, a continuous i.c.v. infusion of saline was initiated (10 µl/h) before recording. The i.c.v. cannula was connected to extended polyethylene tubing attached to an infusion pump through the slip ring with Teflon connecting tubing (0.5 mm inner diameter). Thus, unrestrained movement of the rats was guaranteed during the study. After the rats were acclimatized to the i.c.v. infusion for 1 week, 10 nmol–10 µmol NEM (Sigma, St. Louis, MO, USA) dissolved in saline (100 µl) was infused for 10 h from light onset (08:00). After drug infusion, the saline infusion was continued for 3 days to observe the recovery period. At the end of the experiment, animals were deeply anesthetized with ether and perfused transcardially with 0.9% saline and 4% phosphate-buffered paraformaldehyde. Brains were removed and fixed in paraformaldehyde at 4°C. Coronal sections (60 µm) were cut using a cryostat at −20°C and stained with Cresyl Violet for histological confirmation. The tip of the cannula was found in the third ventricle -1.1 ± 0.3 mm from the bregma in all animals examined.

Immunohistochemistry

A monoclonal antibody (511CA) was generated against rat A1R and characterized previously (Ochiishi et al., 1999a). The 511CA antibody was obtained from culture supernatants of the hybridoma. Twenty day old male Wistar rats (Charles River Japan, Tokyo, Japan) were used for immunohistochemical study. Animals were deeply anesthetized by an i.p. injection of sodium pentobarbital (50 mg/kg body weight) and transcardially perfused with phosphate-buffered saline (PBS) for 5 min and then with ice-cold 4% paraformaldehyde in 0.1 M phosphate buffer for 15 min. The brain tissue was fixed in the same fixative (4°C, 2 h) and immersed in 30% sucrose PBS. Frozen sections of 12 µm thickness were cut with a cryostat microtome and mounted on gelatin-subbed microscope slides. The samples were incubated in 1% goat serum for 1 h to block non-specific labeling and in the hybridoma supernatant (the 511CA antibody) dissolved in 0.02% Triton X-100/PBS overnight at 4°C. For visualization of the immunoreactivity, sections were immersed in 1:200 biotinylated goat anti-mouse IgG (Vector Laboratories, Burlingame, CA, USA) for 1 h, rinsed with PBS, and treated with 1:100 avidin–biotin–peroxidase complex (Vector) for 30 min. The immunoreactivity was visualized with 0.05% 3,3′-diaminobenzidine (Dojin, Osaka, Japan) in Tris–HCl-buffered saline (pH 7.4) containing 0.003% H_2O_2. In addi-

Table 1. Effects of i.c.v. NEM on sleep amount and brain temperature (T_{br}) in the rat

NEM (μmol/10 h)	Light period (08:00–20:00)				Dark period (20:00–08:00)		
	n	NREMS	REMS	T_{br}	NREMS	REMS	T_{br}
0	22	417.8 ± 6.4	70.0 ± 2.5	36.64 ± 0.09	260.7 ± 9.6	26.3 ± 2.7	37.29 ± 0.12
0.01	5	473.9 ± 6.3	66.0 ± 7.3	36.66 ± 0.16	278.8 ± 17.2	31.3 ± 3.5	37.19 ± 0.18
0.1	5	423.8 ± 21.2	67.3 ± 6.7	36.87 ± 0.03	282.2 ± 17.7	29.0 ± 7.0	37.60 ± 0.36
1	6	361.4 ± 13.0*	52.7 ± 6.1**	36.89 ± 0.14	288.6 ± 15.7	47.8 ± 7.7**	37.04 ± 0.10
10	6	178.8 ± 53.5**	7.8 ± 3.1**	37.67 ± 0.22**	347.1 ± 19.5**	94.3 ± 10.5**	37.60 ± 0.24

*$P < 0.05$, **$P < 0.01$ in comparison with the vehicle control by Duncan's multiple range test following one way ANOVA.

tion, confocal microscopy was used to analyze the cellular localization of A1R in the immunopositive brain regions. For the fluorescent measurements, immunoreactivity was visualized with 1:200 fluorescein isothiocyanate-conjugated goat anti-mouse IgG (Cappel, West Chester, PA, USA). The fluorescent images were acquired using a confocal laser-scanning unit (MRC 1024; Bio-Rad, Hertfordshire, UK) mounted on a fluorescent microscope (Axoplan 2 with oil immersion objective 63×/1.4 Plan-Apochromat; Carl Zeiss, Thornwood, NY, USA).

Ca^{2+} imaging

Sprague–Dawley rats (16–22 days old; 50–75 g; Taniac, Germantown, NY, USA) were used for the Ca^{2+} imaging experiments. Coronal hypothalamic slices (200 μm) containing the medial preoptic area were made with a vibrating-blade microtome in ice-cold high Mg^{2+} artificial cerebrospinal fluid (ACSF) containing (mM): 138.6 NaCl, 3.35 KCl, 21 $NaHCO_3$, 0.6 NaH_2PO_4, 9.9 D-glucose, 0.5 $CaCl_2$, and 3 $MgCl_2$, bubbled with 95% O_2/5% CO_2. Sequential slices at approximately bregma −0.3 mm were cut from a rat brain according to the brain map. The slices were incubated for 1–6 h in the ACSF of 2.5 mM $CaCl_2$, and 1 mM $MgCl_2$, bubbled with 95% O_2/5% CO_2 and transferred for 1 h to ACSF containing 10 μM fura-2 AM (Molecular Probe, Eugene, OR, USA) and 0.001% Cremophore El (Sigma) at room temperature. Fluorescent images were obtained with an upright microscope (Axioskop FS; Carl Zeiss) with a water immersion objective (FL40×/0.8, Olympus). The wavelength of the excitation UV light (340 nm or 380 nm pulse of 143 ms) was switched by a monochromator (Polychrome 2; Till Photonics, Martinsried, Germany) and the UV light was reflected by a dichroic mirror (FT 395 nm; Carl Zeiss). The pair of fluorescent images were band-passed (BP 485–515 nm; Carl Zeiss), amplified by an image intensifier (C7039-02; Hamamatsu Photonics, Hamamatsu, Japan) and exposed to a multiple format cooled charge-coupled device camera (C4880; Hamamatsu Photonics) at 6 s intervals. The monochromator and the charge-coupled device camera were controlled by digital imaging software (ARGUS HiSCA; Hamamatsu Photonics). The background fluorescence was subtracted by the imaging system. During the recording, slices were placed in a 0.5 ml bath chamber and perfused with ACSF at a flow rate of 3 ml/

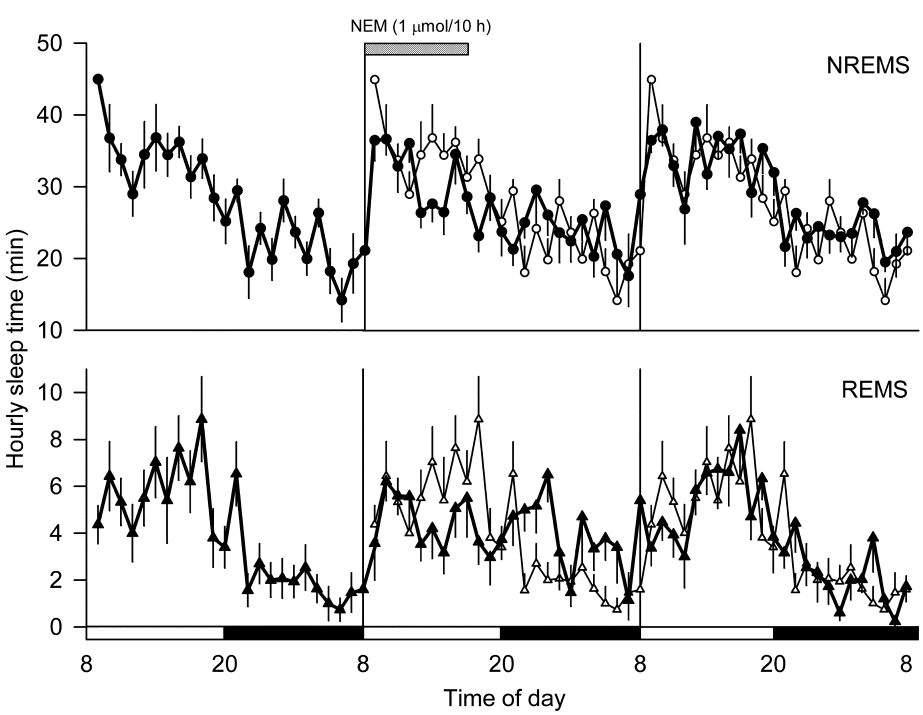

Fig. 1. Effects of continuous i.c.v. infusion of 1 μmol/10 h NEM (as indicated by shadowed bar) on NREMS and REMS in the rat. Continuous vehicle infusion (10 μl/h) was initiated 1 week before the NEM infusion and continued to the end of the experiment. White and black bars on the bottom indicate the light and dark periods, respectively. The control sleep amount before the NEM infusion was superimposed on the plots during the NEM infusion day and recovery day (open circles for NREMS and open triangles for REMS). Error bars indicate S.E.M. $n = 6$. The difference in the cumulative sleep amount was described in Table 1.

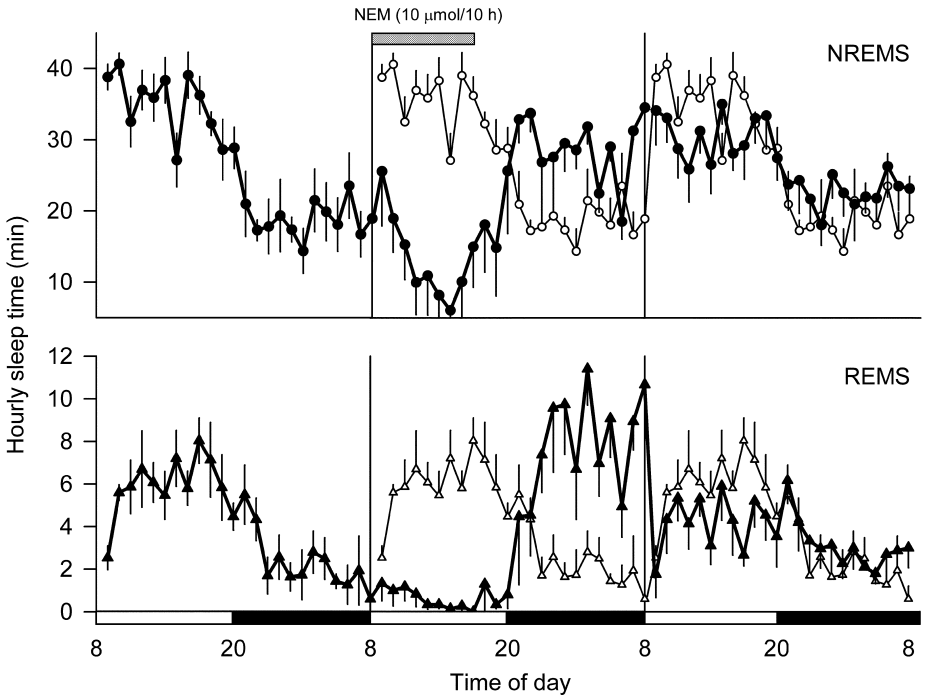

Fig. 2. Effects of continuous i.c.v. infusion of 10 μmol/10 h NEM (as indicated by shadowed bar) on NREMS and REMS in the rat. The control sleep amount was superimposed on the plots during the NEM infusion day and the recovery day (open circles for NREMs and open triangles for REMS). Error bars indicate S.E.M. $n = 6$. The difference in the cumulative sleep amount was described in Table 1. Note the dramatic reduction of NREMS and REMS during the NEM infusion and the compensatory rebound increase of sleep during the subsequent day-time, resulting in a reversed circadian sleep–wake rhythm on the experimental day.

min. The N^6-cyclopentyladenosine (CPA; Sigma), 8-cyclopentyldipropylxanthine (DPCPX; Sigma), NEM, tetrodotoxin (TTX; Alomone labs, Jerusalem, Israel), and 80 mM potassium (high K^+) ACSF were applied by switching the perfusate. Further details of the Ca^{2+} imaging techniques with hypothalamic slices are described elsewhere (Allen et al., 1999; Ikeda et al., 2000b).

Statistical analysis

All data are presented as means with S.E.M. One way analysis of variance (ANOVA) followed by Duncan's multiple range test was used for the statistical comparisons. The 95% confidence level determined statistical significance.

RESULTS

Reduction of diurnal sleep and increase of brain temperature by NEM

During continuous i.c.v. infusion of saline, rats had diurnal rhythms of NREMS and REMS consistent with our recent observations of rat's sleep without i.c.v. infusions (Ikeda et al., 2000a). A 10 h infusion of 10–100 nmol NEM from the onset of the light period did not affect the sleep–wake or brain temperature rhythms (Table 1). Infusion of 1 μmol NEM caused a partial inhibition of NREMS and REMS during the light period (Fig. 1, Table 1) while 10 μmol NEM inhibited both NREMS and REMS with a short latency (< 2 h) (Fig. 2). Notably, both NREMS and REMS were almost completely inhibited 7 h after the maximal dose of NEM (10 μmol/10 h). These results indicate a dose-dependent inhibition of NREMS ($F_{5,39} = 24.31$, $P < 0.001$ by one way ANOVA) and REMS ($F_{5,39} = 28.95$, $P < 0.001$ by one way ANOVA) during the day-time (Table 1). Similar to the effects of NEM on sleep, 10 μmol NEM significantly elevated brain temperature during the light period while the lower concentrations (10 nmol–1 μmol) of NEM had no significant effects on brain temperature (Table 1). After sleep deprivation by 1 or 10 μmol NEM, there was a rebound increase of NREMS ($F_{5,39} = 14.59$, $P < 0.01$ by one way ANOVA) and REMS ($F_{5,39} = 22.88$, $P < 0.001$ by one way ANOVA) during the subsequent dark period. During the subsequent recovery day, no significant changes were observed in NREMS, REMS, or brain temperature.

Localization of A1R-like immunoreactivity in the rat hypothalamus

To explore the principal site and mechanism of NEM actions, we examined immunostaining of A1R with a monoclonal antibody in the rat hypothalamus. At a locus neighboring the cannula, significant immunoreactivity for A1R was detected. In the section at bregma −1.1 mm, robust staining was found in the supraoptic nucleus and the ventral part of the suprachiasmatic nucleus (Fig. 3A, left). In the supraoptic nucleus, the subcellular localization of A1R seems to be dominant on post-synaptic membranes since the antibody preferentially recognized cell bodies (Fig. 3Bc). In rostral sections

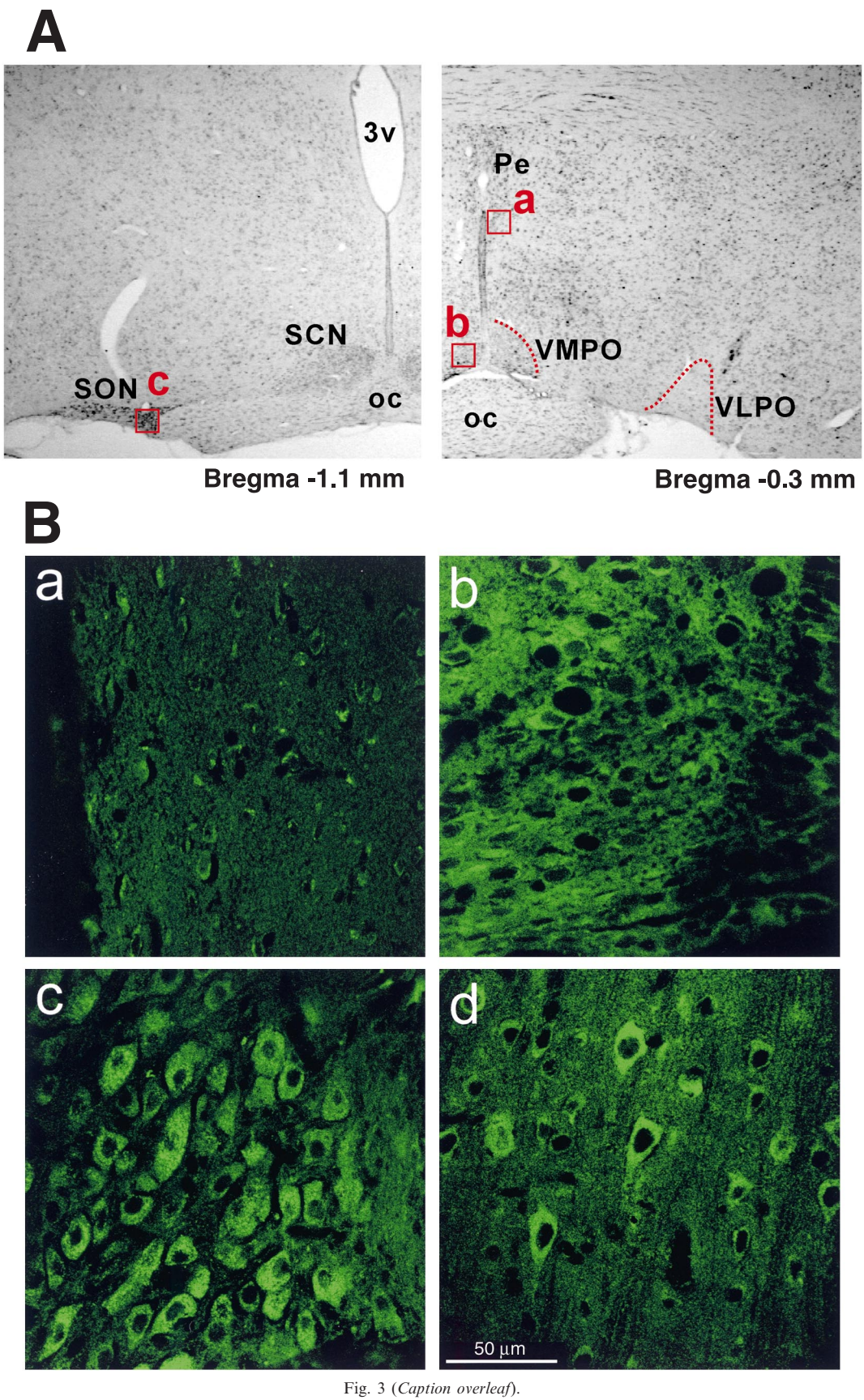

Fig. 3 (*Caption overleaf*).

(bregma −0.3 mm), the medial preoptic area displayed relatively higher staining levels than the lateral part of the preoptic area (Fig. 3A, right) and the VMPO displayed some of the most robust immunoreactivity observed. The subcellular localization appeared to be post-synaptic since immunoreactivity was dominant on the cell bodies of the VMPO (Fig. 3Bb). The periventricular nucleus was stained relatively darker with diaminobenzidine and the confocal microscopy demonstrated immunoreactivity on the small diameter (~10 μm) somas as well as fibers of passage (Fig. 3Ba, identified as bright punctate spots), suggesting pre- and post-synaptic A1R localization. The A1R antibody did not positively stain the ventrolateral preoptic nucleus (VLPO), where sleep-active neurons are localized (Fig. 3A, right).

Effects of A1R regulators and glutamate on the spontaneous Ca^{2+} oscillations in the VMPO

In a ventromedial preoptic slice, 4–11 cells were visualized by fura-2 staining and 40.0 ± 5.3% (number of slices = 23) of the cells had spontaneous Ca^{2+} oscillations. The baseline Ca^{2+} levels and phase of the Ca^{2+} oscillations varied widely among the visualized cells (Fig. 4A). The A1R agonist, CPA (200 nM), inhibited the Ca^{2+} oscillations in 10 out of 24 recorded cells (Fig. 4A). The A1R antagonist, DPCPX (300 nM), induced large amplitude Ca^{2+} oscillations in four of 22 cells and slightly elevated baseline Ca^{2+} levels (Fig. 4B). These results indicate endogenous adenosine release and an inhibitory action of A1R on Ca^{2+} oscillations in the VMPO. A short (< 3 min) NEM (200 μM) application did not significantly alter the Ca^{2+} oscillations or baseline Ca^{2+} levels while a longer (> 6 min) NEM application slightly increased the baseline Ca^{2+} levels in 16 out of 20 cells (data not shown). Glutamate (300 μM) evoked a massive Ca^{2+} increase and high amplitude Ca^{2+} oscillations in the majority of the cells (20 out of 24 cells) (Fig. 4C). Stimulation of glutamate receptors induces an influx of Ca^{2+} through glutamate receptor-linked ion channels, produces membrane depolarization, and activates voltage-sensitive Ca^{2+} channels (VSCCs). Since A1R inhibits VSCCs via $G_{i/o}$ proteins in a NEM-sensitive manner (Barajas-López et al., 1996), we further clarified the effects of CPA, DPCPX, and NEM on high K^+-induced Ca^{2+} flux in the VMPO.

Effects of NEM on A1R-mediated inhibition of high K^+-induced Ca^{2+} flux in the VMPO

The replacement of normal ACSF with high K^+ (80 mM) ACSF induces depolarization and Ca^{2+} influx presumably through VSCCs. In the VMPO, the high K^+-induced Ca^{2+} response (mean fura-2 ratio change = 0.22 ± 0.02, $n = 12$) was reproducible four times at 8 min intervals without significant decay of the responsiveness (Fig. 5A). Application of CPA (200 nM) with the second K^+ stimulation significantly reduced the Ca^{2+} response (−25.3 ± 2.4% of the first K^+ response, $n = 29$, $P < 0.01$ by Duncan's multiple range test) and the effect of CPA washed out during the third and fourth Ca^{2+} responses (Fig. 5B, G). The effect of CPA was not significantly reduced by continuous perfusion of 1 μM TTX ($P > 0.05$ in comparison with CPA-treated group by Duncan's multiple range test, $n = 13$) (Fig. 5G), suggesting little contribution of synaptic transmission to CPA actions. DPCPX (300 nM, $P < 0.05$ by Duncan's multiple range test, $n = 24$) (Fig. 5C, G) and NEM (100 μM, $P < 0.01$ by Duncan's multiple range test, $n = 23$) (Fig. 5D, G) blocked CPA's action and increased the K^+-induced Ca^{2+} response (+7.8 ± 2.5%, $P < 0.05$ for DPCPX-supplemented group and +13.4 ± 3.0%, $P < 0.01$ for the 100 μM NEM group). Interestingly, a higher concentration (200–300 μM) of NEM increased the K^+-induced Ca^{2+} responses as well as the baseline Ca^{2+} levels and the effect did not recover within the recording period (Fig. 5E, F). These results indicate that the A1R antagonist, DPCPX, as well as the $G_{i/o}$ protein uncoupler, NEM, blocked the A1R-mediated inhibition of Ca^{2+} signaling and increased the Ca^{2+} influx presumably through the VSCCs in the VMPO.

DISCUSSION

Various sleep-promoting substances, including neurotransmitters, hormones, neuron growth factors, and cytokines, regulate sleep–wake activities (for reviews Inoué et al., 1985; Inoué, 1986; Krueger et al., 1999). Since sleep regulatory systems are complex, complete sleep disruption by agonists and/or antagonists has not been described. Here, we examined the i.c.v. infusion of NEM and observed almost complete but reversible inhi-

Fig. 3. Distribution of A1R-like immunoreactivity in the rat hypothalamus. (A) Macroscopic distribution of A1R was visualized with a monoclonal antibody against A1R. A hypothalamic section at bregma −1.1 mm (left) demonstrated positive staining of the supraoptic nucleus (SON) and the ventral part of the suprachiasmatic nucleus (SCN). oc: optic chiasma. 3v: third ventricle. The section at bregma −0.3 mm (right) showed positive staining in the periventricular nucleus (Pe) and VMPO while little staining was found in the VLPO where sleep-active neurons located. (B) Distribution of staining in each immunopositive area (a–c, the approximate area was shown in A) was analyzed using a fluorescein isothiocyanate-labeling secondary antibody and confocal microscopy. (a) The periventricular nucleus displays immunoreactivity in small (diameter = 5–10 μm) somata and fiber-like spots. (b) The VMPO displayed A1R-like immunoreactivity on the cell bodies (diameter = 10–40 μm). (c) Robust staining was found on the cell bodies of supraoptic nucleus neurons. (d) Control staining of somatosensory cortex neurons (located in the same section containing the area shown in c) displayed heterologous distribution of A1R immunoreactivity. The selective staining indicates the successful preparation of the monoclonal antibody and immunostaining.

bition of NREMS and REMS. The potency of the effects of NEM on sleep regulation was dramatic compared to the effects of other sleep-promoting substances studied using the same i.c.v. infusion strategy (Inoué et al., 1984; Honda et al., 1984, 1994, 2000; Kimura et al., 2000). The results provide a novel experimental model to produce sleep deprivation with a chemical compound.

NEM will diffuse throughout the CNS via cerebrospinal fluid flow and thus the present study does not identify the site of action of NEM or the mechanism by which NEM disrupts sleep. NEM is lipophilic and may diffuse from the periventricular area to the lateral preoptic area in a dose-dependent manner. Since the maximal dose of NEM tested (10 μmol/10 h) did not damage the periventricular nucleus or medial preoptic area where the cannula was located, the mechanism of sleep disturbance is different from that caused by the brain lesions. Since the NEM action was rapid and reversible, it is likely that the neuronal circuits located near the third ventricle may be involved in the transient sleep disturbance. Among several possible brain sites, the hypothalamic preoptic area may be the most likely. Lesions of the preoptic area induced a significant reduction of NREMS and REMS with an increase of body temperature levels in rats and cats (Sallanon et al., 1989; Asala et al., 1990; John and Kumar, 1998). The medial preoptic area contains thermo-sensitive neurons whose discharge frequency is dependent both on the temperature and sleep status (Alam et al., 1995). In addition, Lu et al. (2000) recently reported that lesions of the VLPO, containing sleep-active neurons (Sherin et al., 1996), produce a long-lasting insomnia in the rat with little effect on body temperature, while lesions of the VMPO produce hyperthermia with relatively small effects on sleep–wake activities. Since NEM permeates from the medial to the lateral preoptic area and affects both brain temperature and sleep–wake activities, one possible action of i.c.v. NEM may be blocking of neuronal signaling in the medial preoptic area or the neuronal circuit regulating the VLPO.

It has been suggested that multiple NEM-sensitive $G_{i/o}$ protein-coupled receptors may regulate sleep and wakefulness. For example, M2 muscarinic receptors (coupled to $G_{i/o}$) but not M1 or M3 receptors (coupled to G_{q11}) in the medial preoptic area were reported to modulate NREMS and cortical temperature (Imeri et al., 1996). The sleep-active neurons in the VLPO are characterized by immunoreactivity against galanin and glutaminic acid decarboxylase and these neurons project to arousal-related histaminergic neurons in the hypothalamic tuberomammillary nucleus (Sherin et al., 1998; Gallopin et al., 2000). Since most subtypes of the galanin receptor couple to $G_{i/o}$ proteins, this pathway should be NEM-sensitive. Adenosine is one of the most potent sleep promoters in rats and cats (Virus et al.,

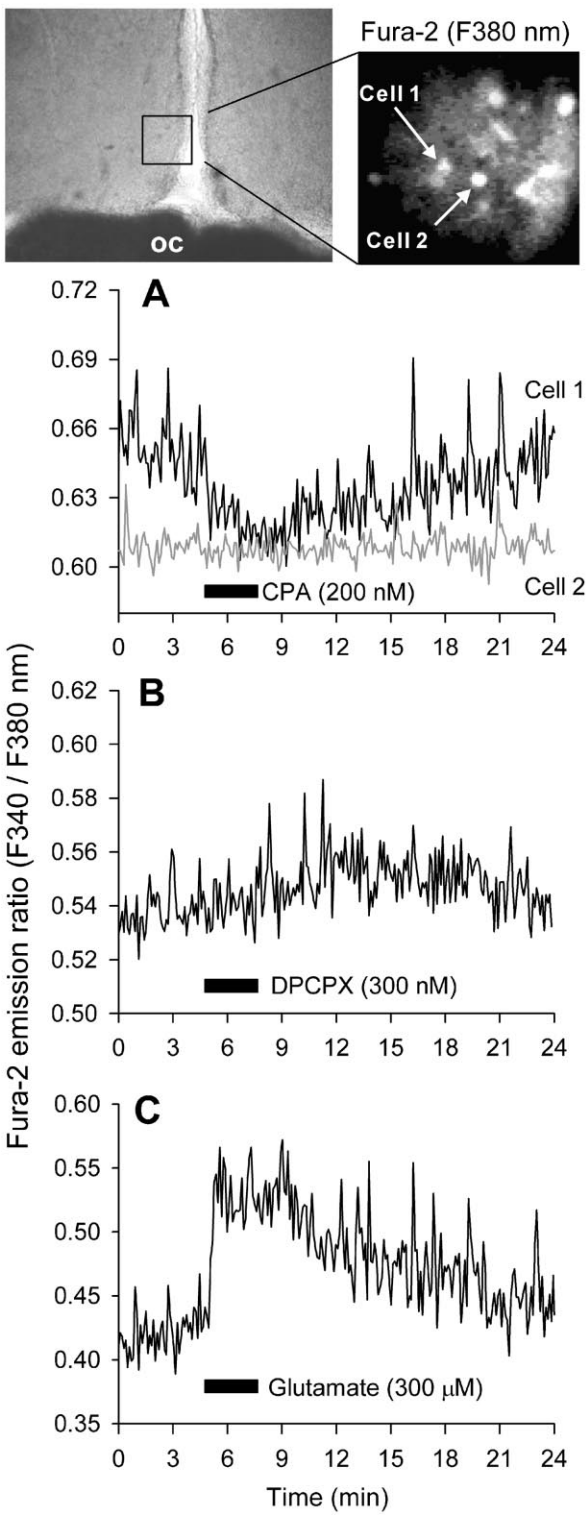

Fig. 4. An image of the VMPO by transmitted light (left) and the fura-2 fluorescent image (right) excited by 380 nm UV light (F380 nm). (A) An example time course of changes in intracellular Ca^{2+} analyzed in two individual cells. Cell 1 displayed spontaneous Ca^{2+} oscillations and stimulation of the A1R by CPA inhibited the Ca^{2+} oscillations. CPA had no effect on cell 2 (gray line), suggesting that CPA inhibited intracellular Ca^{2+} oscillations in a subpopulation of VMPO cells. (B) The A1R antagonist, DPCPX, evoked Ca^{2+} oscillations and slightly increased the baseline Ca^{2+} levels in a subpopulation of VMPO cells. (C) Glutamate also evoked a massive increase of Ca^{2+} and high amplitude Ca^{2+} oscillations in the majority of ventromedial preoptic cells. The similar Ca^{2+} responses were repeatedly observed in at least four individual cells.

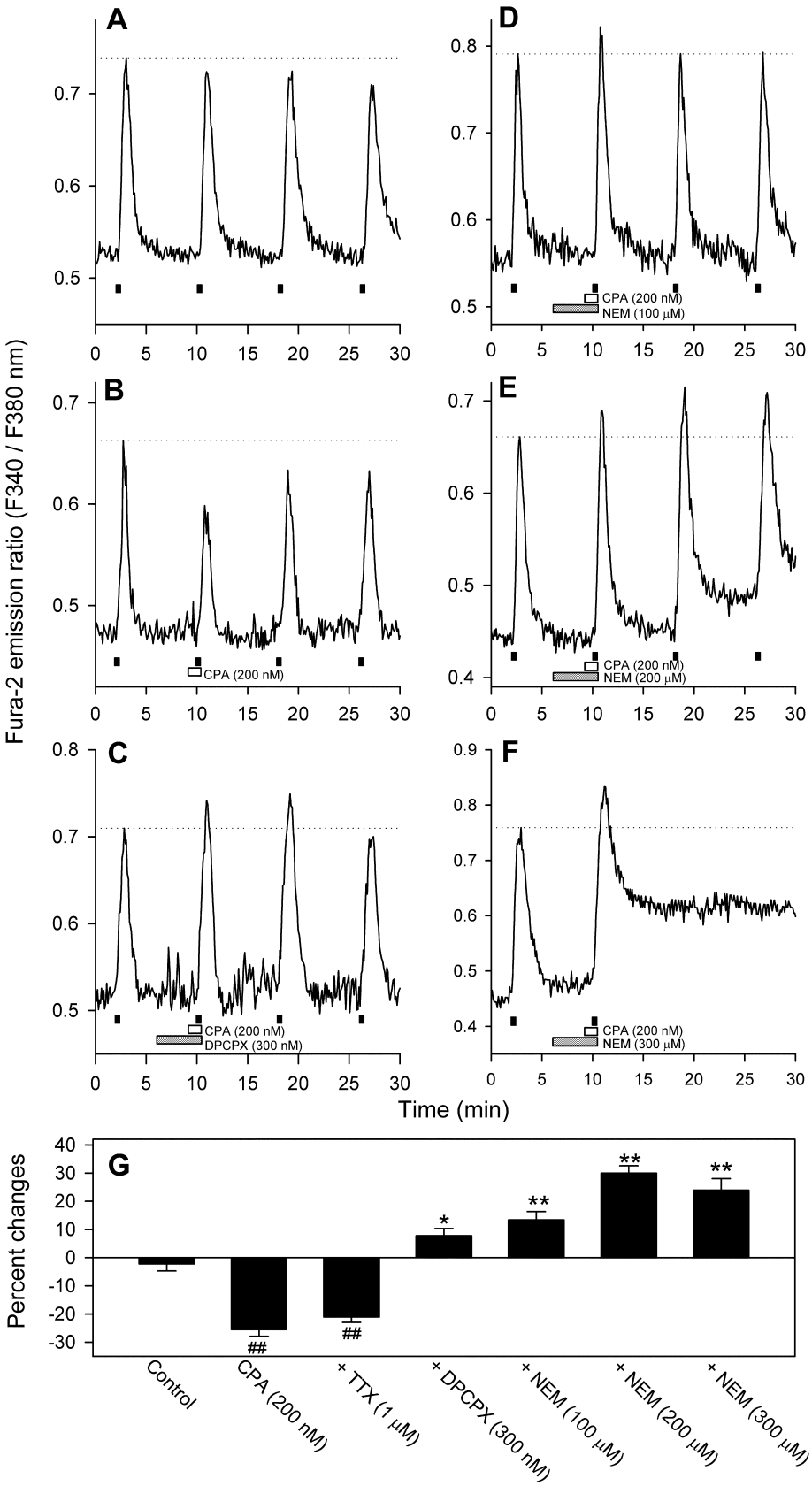
A
B
C
D
E
F
G
Fura-2 emission ratio (F340 / F380 nm)
Time (min)
CPA (200 nM)
DPCPX (300 nM)
NEM (100 μM)
NEM (200 μM)
NEM (300 μM)
Percent changes
Control
CPA (200 nM)
+ TTX (1 μM)
+ DPCPX (300 nM)
+ NEM (100 μM)
+ NEM (200 μM)
+ NEM (300 μM)
##
*
**

Fig. 5.

1983; Portas et al., 1997). The inhibitory action of adenosine on cortical acetylcholine that is linked to the sleep EEG is mediated by $G_{i/o}$-coupled A1R but not by the G_s-coupled A2a adenosine receptor (Materi et al., 2000). In addition, an A1R agonist but not an A2a adenosine receptor agonist injected into the preoptic area increased sleep and reduced brain temperature (Ticho and Radulovacki, 1991). These reports suggest that NEM-sensitive $G_{i/o}$-coupling receptors play an important role in sleep and body temperature regulation.

Although adenosine is present widely in the CNS and the release is dependent on the general level of neuronal activity (Mitchell et al., 1993; Manzoni et al., 1994), the details of the receptor localization and functioning are still poorly understood. After the successful cloning of A1R (Mahan et al., 1991; Reppert et al., 1991), the widespread localization of A1R mRNA was visualized using *in situ* hybridization. However, the distribution of the functional receptor protein visualized with monoclonal antibody-based immunohistochemistry was more localized than the mRNA in the hippocampus (Ochiishi et al., 1999a). Therefore, we used the antibody against A1R (Ochiishi et al., 1999a,b) to visualize A1R in the hypothalamus. The present results demonstrate A1R-like immunoreactivity in the periventricular nucleus, the medial preoptic area, the suprachiasmatic nucleus, and the supraoptic nucleus. A1R agonists induce pre-synaptic inhibition of neurotransmitter release in the supraoptic nucleus (Oliet and Poulain, 1999). However, the present results demonstrate the distribution of A1R on the cell bodies of supraoptic nucleus and suggest its possible localization at post-synaptic sites (Noguchi and Yamashita, 2000). Interestingly, high-density immunoreactive cell bodies were found in the VMPO while little immunoreactivity was found in the VLPO. The results provide a reasonable interpretation of the adenosine action in the preoptic area, since elevated extracellular adenosine at the onset of sleep (Porkka-Heiskanen et al., 1997) may not directly inhibit the sleep-active neurons located in the VLPO.

To analyze the cellular functions of A1R in the VMPO, we used fura-2-based Ca^{2+} imaging together with acute hypothalamic slices. Similar experiments used dispersed cell cultures of hypothalamic neurons to analyze the function of A1R (Obrietan et al., 1995). Baseline Ca^{2+} levels and spontaneous Ca^{2+} oscillations in the VMPO were increased by glutamate and suppressed by the A1R agonist, CPA (Fig. 4A, C). We previously demonstrated that the extracellular glutamate concentration in the medial preoptic area was elevated during the arousal state (Azuma et al., 1996). Together with the present results, we suggest that the intracellular Ca^{2+} concentrations in the VMPO neurons may be coupled to the sleep–wake state, although neuronal activities and intracellular Ca^{2+} mobilization may not be equivalent between *in vivo* and *in vitro* preparations. The A1R antagonist, DPCPX, activated Ca^{2+} oscillations (Fig. 4B), suggesting an endogenous release of adenosine and steady-state inhibition of intracellular Ca^{2+} in VMPO neurons. In addition, a K^+-induced Ca^{2+} flux was reduced by the A1R agonist, CPA, and increased by the signaling blockers, DPCPX and NEM. These results indicate that VSCCs in the VMPO neurons undergo A1R regulation. The CPA action was TTX-insensitive and thus A1R may regulate VSCCs post-synaptically, consistent with the post-synaptic receptor localization observed with immunohistochemistry. The relatively stronger effects of NEM compared to DPCPX may suggest involvement of other $G_{i/o}$-coupled receptors in the inhibition of VSCCs in the VMPO neurons. Hence, we demonstrate that the intracellular Ca^{2+} concentration in the VMPO neurons is regulated by A1R and may be related to the sleep–wake states and body temperature levels.

Other possible effects of NEM on neuronal activity may be mediated by the inhibition of NEM-sensitive enzymes and these effects still remain to be characterized. NEM inhibits protein phosphatase activity (Cossins et al., 1994; Clottes and Burchell, 1998) and inhibition of phosphatase by NEM eventually modulates a Na^+–K^+–$2Cl^-$ cotransporter activity in turkey red cells (Muzyamba et al., 1999). Therefore, we need to clarify the effects of phosphatase inhibitors in the regulation of sleep and wakefulness. NEM and a sulphydryl reagent, selenium tetrachloride, have been used as blockers of glutathione peroxidase (Preclik et al., 1992) and prostaglandin D_2 synthase (Islam et al., 1991), respectively. The products of these enzymes, oxidized glutathione and prostaglandin D_2, are endogenous sleep inducers (Honda et al., 1994, 2000; Matsumura et al., 1994). Therefore, i.c.v. NEM may modulate sleep partially via alteration of the activities of these enzymes. Matsumura et al. (1991) observed that i.c.v. infusion of selenium tetrachloride significantly decreased NREMS and REMS and concluded that the effect was produced via inhibition of prostaglandin D_2 synthase. However, the amount of sleep inhibited by NEM or selenium tetrachloride was apparently larger than that enhanced by oxidized glutathione or prostaglandin D_2, and thus further characterizations were needed to clarify the causal

Fig. 5. (A) Stimulation of the VMPO area with high K^+ (80 mM for 30 s, shown as closed square) induced a Ca^{2+} elevation and the response was reproducible at 8 min intervals. (B) Application of CPA (200 nM) significantly reduced a subsequent high K^+-induced Ca^{2+} elevation. (C) Application of DPCPX (300 nM) with CPA blocked the CPA action and slightly increased the high K^+-induced Ca^{2+} elevation. (D–F) NEM (100–300 μM) inhibited CPA actions and increased the high K^+-induced Ca^{2+} elevation. Note that higher concentrations of NEM (200–300 μM) induced a long-lasting increase of baseline Ca^{2+} levels. (G) The mean of relative changes of high K^+-induced Ca^{2+} elevation (the first high K^+ response was regarded as 100%) was plotted with S.E.M. $n = 6$–29 for each group. Since the second high K^+ peaks were slightly smaller than the first high K^+ response without any drugs, the control response displays a negative mean value. The means of the CPA-treated group and the TTX (1 μM)-supplemented group were not statistically different. $F_{6,116} = 54.91$, $^{\#\#}P < 0.01$ in comparison with control group, $^{*}P < 0.05$, $^{**}P < 0.01$ in comparison with CPA-treated group by Duncan's multiple range test following one way ANOVA.

relationships. Here we examined one possible action of sulphydryl reagents on neuronal activity in hypothalamic slices and demonstrate that A1R-mediated neuronal signaling in the VMPO is sensitive to NEM.

CONCLUSION

The present results demonstrate that the sulphydryl reagent, NEM, in the third ventricle significantly reduced NREMS and REMS with increase of brain temperature. One of the possible NEM actions on sleep regulatory neurons may be mediated by the blockade of A1R functions in the VMPO, where NEM-sensitive A1R and endogenous adenosine release were abundant. Although other NEM-sensitive sleep-inhibitory pathways are still remaining to be characterized, our results suggest that NEM-sensitive $G_{i/o}$-coupling receptors are important for the induction of sleep and regulation of body temperature in the rat.

Acknowledgements—We thank Drs. S. Tanaka and Y. Ren (Gunma University) for their excellent technical assistance with the immunostaining assays. We also thank Dr. J. Noguchi (University of Occupational and Environmental Health) for his helpful comments on this manuscript. This work is supported in part by a grant from 'Research for the Future (RFTF)' program 96L00310 from Japan Society for the Promotion of Science to T.Y., a Grant from the NIH (NS036607) to C.N.A., a grant from Ono pharmaceutical company to C.N.A., M.I., and T.Y., and a Special Coordination Fund for Promoting Science and Technology from the Science and Technology Agency, Prime Minister's Office to S.I.

REFERENCES

Alam, M.N., McGinty, D., Szymusiak, R., 1995. Neuronal discharge of preoptic/anterior hypothalamic thermosensitive neurons: relation to NREM sleep. Am. J. Physiol. 269, R1240–R1249.

Alam, M.N., Szymusiak, R., Gong, H., King, J., McGinty, D., 1999. Adenosinergic modulation of rat basal forebrain neurons during sleep and waking: neuronal recording with microdialysis. J. Physiol. Lond. 521, 679–690.

Allen, C.N., Jiang, Z.-G., Teshima, K., Darland, T., Ikeda, M., Nelson, C.S., Quigley, D.I., Yoshioka, T., Allen, R.G., Rea, M.A., Grandy, D.K., 1999. Orphanin-FQ/nociceptin (OFQ/N) modulates the activity of suprachiasmatic nucleus neurons. J. Neurosci. 19, 2152–2160.

Asala, S.A., Okano, Y., Honda, K., Inoué, S., 1990. Effects of medial preoptic area lesion on sleep and wakefulness in unrestrained rats. Neurosci. Lett. 114, 300–304.

Asano, T., Ogasawara, N., 1985. Uncoupling of γ-aminobutyric acid B receptors from GTP-binding proteins by *N*-ethylmaleimide: Effect of *N*-ethylmaleimide on purified GTP-binding proteins. Mol. Pharmacol. 29, 244–249.

Azuma, S., Kodama, T., Honda, K., Inoué, S., 1996. State-dependent changes of extracellular glutamate in the medial preoptic area in freely behaving rats. Neurosci. Lett. 214, 179–182.

Barajas-López, C., Andrea, L.P., Espinosa-Luna, R., 1996. Cellular mechanisms underlying adenosine actions on cholinergic transmission in enteric neurons. Am. J. Physiol. 271, C264–C275.

Bjorvatn, B., Fagerland, S., Eid, T., Ursin, R., 1997. Sleep/waking effects of selective 5-HT1A receptor agonist given systemically as well as perfused in the dorsal raphe nucleus in rats. Brain Res. 770, 81–88.

Clottes, E., Burchell, A., 1998. Three thiol groups are important for the activity of the liver microsomal glucose-6-phosphatase system. J. Biol. Chem. 273, 19391–19397.

Cossins, A.R., Weaver, Y.R., Lykkeboe, G., Nielsen, O.B., 1994. Role of protein phosphorylation in control of K^+ flux pathways of trout red blood cells. Am. J. Physiol. 267, C1641–C1650.

Delmas, P., Gola, M., 1997. Exotoxin-insensitive G proteins mediate synaptically evoked muscarinic sodium current in rabbit sympathetic neurons. J. Physiol. Lond. 498, 627–640.

Gallopin, T., Patrice, F., Eggermann, E., Cauli, B., Luppi, P.H., Rossier, J., Audinat, E., Mühlethaler, M., Serafin, M., 2000. Identification of sleep-promoting neurons *in vitro*. Nature 404, 992–995.

Garzon, J., Lerida, M., Ulibarri, I., Sanchez-Blazquez, P., 1990. Effect of ICV pertussis toxin and *N*-ethylmaleimide on the levels of substance P and serotonin in brain and spinal cord of the rat. Life Sci. 46, 1217–1222.

Honda, K., Komoda, Y., Nishida, S., Nagasaki, H., Higashi, A., Uchizono, K., Inoué, S., 1984. Uridine as an active component of sleep-promoting substance: its effects on nocturnal sleep in rats. Neurosci. Res. 4, 243–252.

Honda, K., Komoda, Y., Inoué, S., 1994. Oxidized glutathione regulates physiological sleep in unrestrained rats. Brain Res. 636, 253–258.

Honda, K., Sagara, M., Ikeda, M., Inoué, S., 2000. Reduced glutathione regulates sleep in unrestrained rats by producing oxidized glutathione. Sleep Hypn. 2, 26–30.

Ikeda, M., Sagara, M., Inoué, S., 2000a. Continuous exposure to dim illumination uncouples temporal patterns of sleep, body temperature, locomotion and drinking behavior in the rat. Neurosci. Lett. 279, 185–189.

Ikeda, M., Sugiyama, T., Suzuki, K., Moriya, T., Shibata, S., Katsuki, M., Allen, C.N., Yoshioka, T., 2000b. PLC-β4-independent Ca^{2+} rise via muscarinic receptors in the mouse suprachiasmatic nucleus. Neuroreport 11, 907–912.

Imeri, L., Bianchi, S., Angeli, P., Mancia, M., 1996. Muscarinic receptor subtypes in the medial preoptic area and sleep–wake cycles. Neuroreport 7, 417–420.

Inoué, S., 1986. Sleep and sleep substances. Brain Dev. (Review) 8, 469–473.

Inoué, S., Honda, K., Komoda, Y., Uchizono, K., Ueno, R., Hayaishi, O., 1984. Differential sleep-promoting effects of five sleep substances nocturnally infused in unrestrained rats. Proc. Natl. Acad. Sci. USA 81, 6240–6244.

Inoué, S., Honda, K., Komoda, Y., 1985. Sleep-promoting substances. In: Wauquier, A., Gaillard, J.M., Monti, J., Radulovacki, M. (Eds.), Sleep: Neurotransmitters and Neuromodulators. Raven, New York, pp. 305–318.

Islam, F., Watanabe, Y., Mori, H., Hayaishi, O., 1991. Inhibition of rat brain prostaglandin D synthase by inorganic selenocompounds. Arch. Biochem. Biophys. 289, 161–166.

John, J., Kumar, V.M., 1998. The effects of NMDA lesion of medial preoptic neurons on sleep and other functions. Sleep 21, 587–598.

Kimura, M., Kodama, T., Aguila, M.C., Zhang, S.Q., Inoué, S., 2000. Granulocyte-macrophage colony-stimulating factor modulates rapid eye movement (REM) sleep and non-REM sleep in rats. J. Neurosci. 20, 5544–5551.

Krueger, J.M., Obal, F., Jr., Fang, J., 1999. Humoral regulation of physiological sleep: cytokines and GHRH. J. Sleep Res. (Review) 1, 53–59.

Lorenzen, A., Lang, H., Schwabe, U., 1998. Activation of various subtypes of G-protein α subunits by partial agonists of the adenosine A1 receptor. Biochem. Pharmacol. 56, 1287–1293.

Lu, J., Greco, M.A., Shiromani, P., Saper, C.B., 2000. Effect of lesions of the ventrolateral preoptic nucleolus on NREM and REM sleep. J. Neurosci. 20, 3830–3842.
Mahan, L., McVittie, L.D., Smyk-Randall, E.M., Nakata, H., Monsma, F.J., Green, C.R., Sibley, D.R., 1991. Cloning and expression of A1-adenosine receptor from rat brain. Mol. Pharmacol. 40, 1–7.
Manzoni, O.J., Manabe, T., Nicoll, R.A., 1994. Release of adenosine by activation of NMDA receptors in the hippocampus. Science 265, 2098–2101.
Marks, G.A., Birabil, C.G., 1998. Enhancement of rapid eye movement sleep in the rat by cholinergic and adenosinergic agonists infused into the pontine reticular formation. Neuroscience 1, 29–37.
Marks, G.A., Birabil, C.G., 2000. Infusion of adenylyl cyclase inhibitor SQ22,536 into the medial pontine reticular formation of rats enhances rapid eye movement sleep. Neuroscience 98, 311–315.
Materi, L.M., Rasmusson, D.D., Semba, K., 2000. Inhibition of synaptically evoked cortical acetylcholine released by adenosine: an *in vivo* microdialysis study in the rat. Neuroscience 97, 219–226.
Matsumura, H., Takahata, R., Hayaishi, O., 1991. Inhibition of sleep in rats by inorganic selenium compounds, inhibitors of prostaglandin D synthase. Proc. Natl. Acad. Sci. USA 88, 9046–9050.
Matsumura, H., Nakajima, T., Osaka, T., Satoh, S., Kawase, K., Kubo, E., Kantha, S.S., Kasahara, K., Hayaishi, O., 1994. Prostaglandin D2 sensitive sleep-promoting zone defined in the ventral surface of the rostral basal forebrain. Proc. Natl. Acad. Sci. USA 91, 11998–12002.
Mendelson, W.B., 2000. Sleep-inducing effects of adenosine microinjections into the medial preoptic area are blocked by flumazenil. Brain Res. 852, 479–481.
Mitchell, J.B., Lupica, C.R., Dunwiddie, T.V., 1993. Activity-dependent release of endogenous adenosine modulates synaptic responses in the rat hippocampus. J. Neurosci. 13, 3439–3447.
Monti, J.M., Jantos, H., 1992. Dose-dependent effects of the 5-HT1A receptor agonist 8-OH-DPAT on sleep and wakefulness in the rat. J. Sleep Res. 3, 169–175.
Munshi, R., Pang, I.-H., Sternweis, P.C., Linden, J., 1991. A1 adenosine receptors of bovine brain coupled to guanine nucleotide-binding proteins G_{i1}, G_{i2}, and G_o. J. Biol. Chem. 266, 22285–22289.
Muzyamba, M.C., Cossins, A.R., Gibson, J.S., 1999. Regulation of Na^+–K^+–$2Cl^-$ cotransport in turkey red cells: the role of oxygen tension and protein phosphorylation. J. Physiol. Lond. 517, 421–429.
Nagel, J.A., Satinoff, E., 1980. Mild cold exposure increases survival in rats with medial preoptic lesions. Science 208, 301–303.
Noguchi, J., Yamashita, H., 2000. Adenosine inhibits voltage-dependent Ca^{2+} currents in rat dissociated supraoptic neurones via A_1 receptors. J. Physiol. Lond. 526, 313–326.
Obrietan, K., Belousov, A.B., Heller, H.C., van den Pol, A.N., 1995. Adenosine pre- and postsynaptic modulation of glutamate-dependent calcium activity in hypothalamic neurons. J. Neurophysiol. 74, 2150–2162.
Ochiishi, T., Chen, L., Yukawa, A., Saitoh, Y., Sekino, Y., Arai, T., Nakata, H., Miyamoto, H., 1999a. Cellular localization of adenosine A1 receptors in rat forebrain: immunohistochemical analysis using adenosine A1 receptor-specific monoclonal antibody. J. Comp. Neurol. 411, 301–316.
Ochiishi, T., Saitoh, Y., Yukawa, A., Saji, M., Ren, Y., Shirao, T., Miyamoto, H., Nakata, H., Sekino, Y., 1999b. High level of adenosine A1 receptor-like immunoreactivity in the CA2/CA3a region of the adult rat hippocampus. Neuroscience 93, 955–967.
Oliet, S.H., Poulain, D.A., 1999. Adenosine-induced presynaptic inhibition of IPSCs and EPSCs in rat hypothalamic supraoptic nucleus neurones. J. Physiol. Lond. 520, 815–825.
Porkka-Heiskanen, T., Strecker, R.E., Thakkar, M., Bjorkum, A.A., Greene, R.W., McCarley, R.W., 1997. Adenosine: a mediator of the sleep-inducing effects of prolonged wakefulness. Science 276, 1265–1268.
Portas, C.M., Thakkar, M., Rainnie, D.G., Greene, R.W., McCarley, R.W., 1997. Role of adenosine in behavioral state modulation: a microdialysis study in the freely moving cat. Neuroscience 79, 225–235.
Preclik, G., Stange, E.F., Ditschuneit, H., 1992. Limited utilization of exogenous arachidonic acid by the prostaglandin cyclooxygenase in gastric mucosa: the role of protein binding, glutathione peroxidase, and hydrogen peroxides. Prostaglandins 44, 177–197.
Reppert, S.M., Weaver, D.R., Stehle, J.H., Rivkees, S.A., 1991. Molecular cloning and characterization of rat A1-adenosine receptor that is widely expressed in brain and spinal cord. Mol. Endocrinol. 5, 1037–1048.
Sallanon, M., Denoyer, M., Kitahama, K., Aubert, C., Gay, N., Jouvet, M., 1989. Long-lasting insomnia induced by preoptic neurons lesions and its transient reversal by muscimol injection into the posterior hypothalamus in the cat. Neuroscience 32, 669–683.
Sánchez-Blázquez, P., Ulibarri, I., Garzón, J., 1989. Intracerebroventricular *N*-ethylmaleimide differentially reduces supraspinal opioid analgesia in mice. Eur. J. Pharmacol. 166, 193–200.
Schwierin, B., Borbely, A.A., Tobler, I., 1996. Effects of N_6-cyclopentyladenosine and caffeine on sleep regulation in the rat. Eur. J. Pharmacol. 300, 163–171.
Shapiro, M.S., Wollmuth, L.P., Hille, B., 1994. Modulation of Ca^{2+} channels by PTX-sensitive G proteins is blocked by *N*-ethylmaleimide in rat sympathetic neurons. J. Neurosci. 14, 7109–7116.
Sherin, J.E., Shiromani, P.J., McCarley, R.W., Saper, C.B., 1996. Activation of ventrolateral preoptic neurons during sleep. Science 271, 216–219.
Sherin, J.E., Elmquist, J.K., Torrealba, F., Saper, C.B., 1998. Innervation of histaminergic tuberomammillary neurons by GABAergic and galaninergic neurons in the ventrolateral preoptic nucleus of rat. J. Neurosci. 18, 4705–4721.
Tang, K.-C., Lovinger, D.M., 2000. Role of pertussis toxin-sensitive G proteins in synaptic transmisson and plasticity at corticostriatal synapses. J. Neurophysiol. 83, 60–69.
Ticho, S.R., Radulovacki, M., 1991. Role of adenosine in sleep and temperature regulation in the preoptic area of rats. Pharmacol. Biochem. Behav. 40, 33–40.
Virus, R.M., Djuricic-Nedelson, M., Radulovacki, M., Green, R.D., 1983. The effects of adenosine and 2′-deoxycoformycin on sleep and wakefulness in rats. Neuropharmacology 22, 1401–1404.
Williams, S., Mauro, S., Muhlethaler, M., Bernheim, L., 1997. Facilitation of N-type calcium current is dependent on the frequency of action potential-like depolarizations in dissociated cholinergic basal forebrain neurons of the guinea pig. J. Neurosci. 17, 1625–1632.
Winslow, J.W., Bradley, J.D., Smith, J.A., Neer, E.J., 1987. Reactive sulfhydryl groups of α39, a guanine nucleotide-binding protein from brain. J. Biol. Chem. 262, 4501–4507.

(*Accepted* 28 *June* 2001)